Flame Acceleration and Transition to Detonation in Benzene-Air Mixtures

R. Knystautas, J.H.S. Lee
Dept. of Mechanical Engineering
McGill University, Montreal, Canada

J. E. Shepherd
Graduate Aeronautical Laboratories
California Institute of Technology, Pasadena, California, USA

A. Teodorczyk
Warsaw University of Technology, Warszawa, Poland

Published in Combustion and Flame, Volume 115, pp. 424-436, 1998.

Full length article

Short title: Detonation in Benzene-Air

Corresponding author:

Joseph E. Shepherd
Aeronautics, MS 105-50
California Institute of Technology
Pasadena, CA 91125
USA
e-mail: *jeshep@galcit.caltech.edu*
Tel: 626 395 3283
Fax: 626 449 2677

Abstract

We report results on flame acceleration and transition to detonation of benzene-air mixtures at room temperature. Flame acceleration experiments were carried out in a 150-mm diameter, 3.6-m long steel tube. The entire length of the tube is filled with circular orifice plates (blockage or obstructed area ratio of 0.43) spaced one diameter apart. The fuel concentration was varied between 1.7% to 5% by volume of benzene in the fuel-air mixture. The three regimes of propagation were observed: (1) a turbulent deflagration with typical flame speeds less than 100 m/s, (2) a "choking" regime with the flame speed corresponding to the speed of sound of the combustion products, 700 to 900 m/s, and (3) a quasi-detonation regime with a wave speed ranging from 50% to 100% of the Chapman-Jouguet value. Transition from turbulent deflagration to the choking regime occurs at an equivalence ratio of $\Phi = 0.65$ (1.79% C_6H_6) and $\Phi = 1.8$ (4.8% C_6H_6) on the lean and rich sides, respectively. Transition from the choking to the quasi-detonation regime is observed when the wave speed exceeds 1450 m/s. Detonation cell widths were measured using a small charge (8 to 50 g) of solid explosive for direct initiation of the detonation in both the 150-mm diameter tube and a larger 300-mm diameter, 18-m long, steel tube. Sooted foils are used for determining the cell size, which was about 66 mm for a stoichiometric composition. A detailed chemical reaction scheme was used to carry out numerical solutions of the idealized ZND model. The cell widths were approximately 20 times larger than the computed reaction zone lengths. The ZND model was used to examine the effects of initial temperature and dilution by steam and nitrogen, and the effects of adding hydrogen. We conclude that the detonation sensitivity of benzene is similar to that of hexane and slightly more sensitive than propane.

Introduction

Explosion hazards in the chemical industry are often the result of uncontrolled releases of hydrocarbons into the atmosphere. Evaluation and mitigation of these hazards require experimental characterization of the explosive characteristics of the particular fuel-air mixtures of importance for a given industry. Extensive research, summarized in Moen [1], has been carried out on the problem of flame acceleration and transition from deflagration-to-detonation (DDT) in clouds of light hydrocarbons in air.

However, relatively little is known about the flame acceleration in mixtures of heavy hydrocarbons and air. In the study by Beeson [2], the detonation cell width λ of hexane and the commercial aviation fuel JP-4 were determined over a range of nitrogen-to-oxygen ratios, i.e., $\beta = N_2/O_2$ and $0 \leq \beta \leq 3.76$. The detonation cell width for both hexane and JP-4 vapor with air ($\beta = 3.76$) at stoichiometric conditions was found to be about 55 mm, similar to that of propane. In the study of Tieszen [3], detonation cell width measurements and computed reaction zone lengths (based on the ZND model) were reported for 22 compounds. Except for methane, stoichiometric, straight-chain alkanes from ethane to decane all have approximately the same detonation cell width, 40 to 50 mm. Substitution of functional groups such as nitro, nitrate, epoxy and ethers significantly decreases the detonation cell width. Saturated ring structures were found to be more sensitive (smaller cell width) than the corresponding straight-chain alkane.

The present study was carried out to improve our knowledge base of explosion behavior of a common aromatic hydrocarbon: benzene. At room temperature (25°C), the vapor pressure of benzene is about 130 mbar. The flammability limits of benzene in air are 1.3% (lean) to 7.9% (rich) benzene by volume in the fuel-air mixture. Therefore, in an accidental liquid spill, the vapor pressure is sufficiently high to form an explosive vapor cloud. Prior to this study, the transition-to-detonation limits and the intrinsic detonation sensitivity of benzene-air mixtures were unknown.

To assess the sensitivity of a given explosive mixture to flame acceleration and transition-to-detonation, an experimental procedure has been developed [4] which consists of measuring the flame speed in cylindrical tubes. The tube diameter is usually between 50 mm and 300 mm, depending on the sensitivity of the mixture, e.g., larger tubes have to be used for less sensitive mixtures. The tubes are filled with obstacles, in the form of circular orifice plates, spaced about one tube diameter apart along the length of the tube to promote turbulent flame acceleration. Ignition is via a weak spark or a pyrotechnic igniter. The flame speed is measured along the length of the tube using ionization gauges.

The sensitivity of a fuel is generally assessed by the existence of different propagation regimes that can be observed in a given tube and obstacle arrangement. The regimes observed for a variety of hydrocarbon-air mixtures are described in Lee et al. [5]. For example, in mixtures near the flammability limits, the flame accelerates to a steady state value of the order of 10-20 m/s. This regime is referred to as the turbulent deflagration regime. As the sensitivity of the mixture is increased (compositions closer to stoichiometric), transition from the turbulent deflagration to the so-called [5] "choking regime" is observed. In this regime, the terminal steady flame speed jumps from few tens of meters

per second to 700 to 900 m/s, which corresponds approximately to the sound speed of the hot combustion products. An analysis of this propagation regime is given by Chue et al. [6], who show that this situation correponds approximately to an idealized one-dimensional CJ deflagration with sonic outflow of the products relative to the flame and zero product velocity relative to the surrounding tube. The observed terminal velocity of the flame represents the highest speed possible without setting up a mean flow in the products [7, 8].

Depending on the sensitivity of the mixture and the tube and orifice diameters, a second abrupt transition to the so-called [9] "quasi-detonation" regime may occur with further increases in sensitivity. In the quasi-detonation regime, the detonation wave speed can range from about one half to close to the corresponding theoretical Chapman-Jouguet value of the mixture. The propagation mechanism of quasi-detonations [10, 11] is governed by shock reflections and diffraction around the obstacles. The mean wave speed is due to the balance between these complex, multi-dimensional proceses and has no simple explanation as in the case of the "choking regime". Local high temperatures associated with shock wave reflection and focusing are able to sustain a detonation-like phenomena at wave velocities substantially lower than the Chapman-Jouguet value. In a normal detonation, the wave generally fails when the velocity drops more than 10% to 15% below the Chapman-Jouguet value [12].

For insensitive mixtures, the choking and quasi-detonation regimes may not occur for a given tube diameter [4]. For example, for methane-air mixtures, the quasi-detonation regime is not observed even in a 300-mm-diameter tube. Increasing the tube diameter usually widens the composition limits for the quasi-detonation regime. Therefore, the composition range over which quasi-detonations can occur is a measure of the flame acceleration and detonation sensitivity of the mixture. The limiting composition at which transition to quasi-detonation occurs has been correlated [4] with the detonation cell width λ. Other aspects of detonation initiation and propagation are also conventionally correlated [13] with the cell width. For this reason, cell-width measurements should always be made in conjunction with flame acceleration and transition-to-detonation tests.

It should be noted that a fourth propagation mode, the "quenching" regime, was also observed. The quenching regime occurs [4] only under special circumstances for insensitive mixtures near the flammability limits, and when the blockage ratio is also high, i.e., the orifice diameter is very small. Under these special conditions, flame propagation can proceed for a short distance after ignition and then the flame quenches itself when the turbulent jet of hot products emerging from the orifice fails to reignite the mixture downstream of the orifice. Since the quenching orifice diameter is generally only a few mm, such high-blockage ratios are usually not encountered in industrial hazard situations.

Experimental Details

The flame acceleration experiments were carried out in a 150-mm-diameter, 3.6-m-long steel tube, with circular orifice plates of blockage ratio $BR = 0.43$. The blockage ratio

is defined as $BR = 1 - (d/D)^2$, where d is the diameter of the hole in the orifice plate and D is the inner diameter of the tube. The orifice plates were spaced one diameter D apart along the entire length of the tube. Our previous studies [4] indicate that the particular blockage ratio and spacing chosen for the present study correspond to the most effective configuration for flame acceleration. The terminal steady flame speed can usually be attained within 3 m, or about 20 orifice spacings (even for the most insensitive composition).

In the present study, the mixture is prepared by the method of partial pressures within the tube. Mixing is achieved by recirculating the mixture with a metal bellows pump. All experiments were carried out at atmospheric pressure and room temperature, nominally 1 atm and 20°C. To check the mixture composition, samples were taken from the tube after mixing and analyzed with a gas chromatograph. The sample analyses agree within the limits of experimental uncertainty ($\pm 0.1\%$) with the partial pressure measurements.

For the flame acceleration studies, ignition of the mixture was achieved via a pyrotechnic chemical igniter of the type used for the ignition of toy rocket motors. Diagnostics consisted of the measurement of the time of arrival of the flame via ionization probes located at intervals between 15 to 50 cm along the tube. The ionization probe signals are recorded on both a data acquisition system interfaced to a computer and a digital oscilloscope.

The experimental procedure consisted of first evacuating the tube to less than 0.1 Torr. The tube was then filled with benzene vapor to the desired partial pressure. Air was then introduced into the tube until the total pressure is 1 atm. The mixture was recirculated by the bellows pumps for about half an hour to achieve thorough mixing. The mixture was then ignited and the flame arrival time at the various ionization probes was recorded. From the time of arrival of the flame at the various probe locations and the probe spacing, an average flame speed can be determined.

Experiments to measure the detonation cell width were carried out in 15-cm-diameter and 30-cm-diameter unobstructed, smooth-walled tubes. The bulk of the experiments were done in the 15-cm-diameter tube which was 3.75-m long. For the more insensitive mixtures near the composition limits, tests were carried out in the larger 30-cm-diameter tube which was 15.2-m long.

Detonation was initiated at one end of the tube via a detonator augmented by a high explosive (HE) booster charger. For the mixtures in the 15-cm diameter tube, an 8 gm HE booster charge was used; for the 30-cm tube it was about 50 gm. The passage of the detonation wave along the tube was monitored via a sequence of ionization probes spaced along the tube. Accurate detonation velocities could be determined in this manner from the time-of-arrival signals. A sooted aluminum foil was inserted prior to evaluation on the inside at the end of the tube opposite to the ignition end. The foil covered most of the inner circumference of the tube and was typically 6-diameters (90 to 180 cm) long. After a shot, the smoked foil was extracted and from the typical traces left by the passing detonation wave, the detonation cell width was determined.

Results

Figure 1 shows the typical flame speed variation with distance along the tube. The regimes of slow deflagration, choking, and quasi-detonation are shown for both benzene and propane-air mixtures. For all compositions, acceleration to a steady state terminal velocity occurs within about 20 tube diameters. The rapidity of the acceleration to steady state depends on both the lateral confinement and the boundary conditions at the ignition end (i.e., open- or closed-end tube). The present case of a rigid, one-dimensional steel tube with the ignition end closed represents the most favorable boundary condition for flame acceleration.

In general, the strength of the ignition source can also play an important role. Perhaps the most effective ignition source (from the point of view of flame acceleration) is the rapid venting of the hot products from a constant volume explosion into the unburned mixture in the form of a large turbulent jet. The high initial burning rate of a large volume of gases pressurizes the products. The subsequent expansion of the products then accelerates the flame to high velocities. In the present study, the pyrotechnic igniter used represents only a mild ignition source.

For a mixture of 1.75% C_6H_6 (Fig. 1), slightly above the lean limit, the flame accelerates to a terminal velocity of about 100 m/s. For more sensitive mixtures away from the limits, the flame accelerates up to 700 to 900 m/s corresponding to the choking regime, or undergoes transition to a quasi-detonation whose velocity is of the order of 1450 m/s. It is interesting to note that the flame trajectories for both the choking and the quasi-detonation regimes are practically identical suggesting that the turbulent flame acceleration mechanisms are the same.

Experiments were first carried out with propane-air mixtures to permit a direct comparison with the data obtained previously [4]. Figure 2 shows the terminal steady state flame velocity of propane plotted against the fuel concentration (or equivalently, the equivalence ratio). Both the choking and the quasi-detonation regimes are recovered in the present experiments. The values of the flame and quasi-detonation velocities obtained are in accord with those obtained previously. The present results for the critical concentration for the transition from the choking to the quasi-detonation regime differ slightly from those obtained previously. However, no attempts have been made in either the previous or the present study to determine these transition limits more precisely. The flame velocity in the choking regime is between 700 and 900 m/s which corresponds to the sound speed of the hot products. The quasi-detonation velocity is, in general, only weakly dependent on the blockage ratio. The transition from the choking regime to the quasi-detonation regime was found to correspond to a cell-width-to-orifice-diameter (λ/d) ratio of the order of unity.

Results for the terminal steady-state flame and quasi-detonation velocities of benzene-air mixtures are shown in Fig. 3. The three regimes of deflagration, choking and quasi-detonation are all observed in the present experiment with the 150-mm-diameter tube. The magnitudes of the flame and detonation velocities in the three regimes are similar to that of propane. Although the theoretical Chapman-Jouguet velocity for benzene is

slightly lower than the corresponding values for propane at the same equivalence ratio, the values of the quasi-detonation velocity for benzene are about the same as those of propane. The transition limits from the choking to the quasi-detonation regime for benzene are 2.4% ($\Phi = 0.88$) on the lean side and 4.3% ($\Phi = 1.6$) on the rich side. The corresponding transition limits observed for propane are 3.5% ($\Phi = 0.86$) on the lean side and 5% ($\Phi = 1.25$) on the rich side. When expressed in terms of equivalence ratio, the quasi-detonation regime spans a large range of composition in benzene than in propane. This is a reflection of the smaller detonation cell sizes for benzene than for propane at the same equivalence ratio in a rich mixture.

A few tests were also carried out to determine the effects of hydrogen addition to lean C_6H_6-air mixtures. The results are shown on Fig. 3. The addition of 1% H_2 had no measureable effect on the limit value for transition to detonation. The addition of 5% H_2 did have a measureable effect. The limit for transition from choking to quasi-detonation shifted from 2.4% to 2.0% C_6H_6. The limit for transition from low speed deflagration to choking shifted from 1.8% to 1.0% C_6H_6. Previous work [14, 15] on hydrogen has shown that significant flame acceleration, i.e., a transition from low-speed deflagration to choking, will not occur in H_2-air mixtures for less than 10% H_2. Our computations indicate (see subsequent discussion and Fig. 12) that no significant change in the cell width will occur and that these effects are simply due to the increased energy release from the added fuel.

The detonation velocities measured in the unobstructed tube experiments carried out to obtain cell widths are also plotted in Fig. 3. The theoretical values were obtained using the STANJAN code [16]. The agreement between the experimental measurements and the theoretical values indicates that direct initiation was achieved without a substantial initiation transient. The detonation cell width is plotted in Figs. 4 and 5. For the 15-cm-diameter tube, the onset of spin was achieved at both ends of the composition spectrum, i.e., $\lambda \sim 450$ mm at 1.4% ($\Phi = 0.522$) and 6.75% ($\Phi = 2.584$) C_6H_6. Only lean mixtures were tested in the larger 30-cm diameter tube. However, the composition range could only be extended down to 1.3% ($\Phi = 0.470$) C_6H_6 due to limitations on the maximum charge (50 gm) of HE that can be used safely in the tube. Detonation initiation at leaner compositions would require a much larger HE charge. For this reason, the spin limit could not be determined in the 30-cm tube.

To compare the relative detonation sensitivity of benzene-air mixtures, measured cell widths [17, 18] for propane-air are displayed in Figs. 4 and 5. Comparing mixtures with the same equivalence ratio, it is evident that the detonation sensitivity of benzene-air and propane-air mixtures on the lean end are virtually identical. For stoichiometric mixtures, the propane cell width is 55 mm and the benzene cell width is 66 mm. However, rich benzene-air mixtures have a much wider detonability range than rich propane-air mixtures. The richest mixture that could be detonated in the 150 mm diam. tube was $\Phi = 2.584$ for benzene-air compared to $\Phi = 1.68$ for propane-air. In Table 2, benzene-air cell size results are compared to other gaseous hydrocarbon and hydrogen fuel-air data. The cell width for stoichiometric benzene-air mixtures is slightly higher than the range of 40 to 55 mm observed for stoichiometric alkane-air mixtures of propane, ethane, octane,

and hexane.

Thus, it may be concluded from the present results that lean benzene-air mixtures are similar in detonation sensitivity to propane and rich mixtures are most sensitive. In terms of detonation cell width and transition form choking to quasi-detonation, benzene is similar to the alkanes such as ethane, butane, etc., with the exception of methane. The equivalence ratio range over which quasi-detonations are observed for benzene is wider than for propane. This is apparently due to the lower cell widths for rich benzene-air mixtures as compared to propane-air. In the choking regime, the flame speed is governed by the thermodynamic state of the products. Since the energetics of benzene and propane mixtures are about the same, the sound speed, and hence the flame speeds are also similar. The transition from the deflagration to the choking regimes mentioned earlier, is governed by the blockage ratio, the energetics and the turbulent burning rate.

Chemical Kinetic Modeling

A detailed chemical reaction mechanism for benzene oxidation has been used to estimate the ideal reaction length Δ_σ using the Zel'dovich-von Neumann-Döring detonation model. A large number of studies (starting with [19] and [20]) have shown that this type of modeling can be used for qualitative and quantitative predictions of the effects of composition and initial conditions on detonation cell width λ.

Reaction Mechanism

A model for benzene oxidation that is useful for detonation reaction zone computations was developed. The model was based on the work of Bittker ([21, 22, 23]). The mechanism uses 39 species: H_2, O_2, H, O, OH, HO_2, H_2O, H_2O_2, HCO, CO, CO_2, CH, CH_2, CH_3, CH_4, CH_2O, CH_3O, C_2H_2, C_2H_3, C_2H, C_2H_4, C_2H_2O, C_2HO, C_3H_2, C_3H_3, C_3H_4, C_4H_2, C_4H_3, C_4H_4, C_4H_5, C_5H_5, C_5H_6, C_5H_5O, C_5H_4OH, C_6H_5, C_6H_6, C_6H_5O, C_6H_5OH, $C_{12}H_{10}$. There are 120 reactions. The reaction rate constants were specified in the modified Arrhenius form. The thermodynamics of each species were either taken from the standard CHEMKIN database [24] or for some hydrocarbon species, Burcat [25] and Burcat and McBride [26] were used.

Initial comparison with STANJAN [16] equilibrium constant volume calculations indicated a $\sim$100 K difference in temperature, 5% difference in pressure and large amounts of C_4H_4 and C_3H_2 predicted by the kinetic computations. These results indicated that the mechanism was not accurately describing thermodynamic equilibrium for these two species. Since these species are an insignificant part of Bittker's mechanism, we simply removed these species and the associated reactions (Bittker [23] reactions No. 23, 28 and 29).

The reaction mechanism and thermodynamics were tested by comparing against the ignition delay shock-tube experiments of Burcat [27]. The modified mechanism gave very good agreement between the final values of composition and thermodynamic state and

the STANJAN equilibrium computation. The ignition delay times were defined using two criteria: the maximum rate of change of temperature dT/dt_{max} and a 5% increase in the pressure. Although the latter was used by Burcat [27] in analyzing his data, we found that the former generally gave better predictions from the numerical model. The results are shown in Figs. 6 to 10. The modified Bittker model gives results which are within a factor of 2 for the worst case. This was judged sufficient to proceed with the rest of the study.

We did examine one other reaction mechanism of Emdee [28], which used 33 species and 130 reactions. This work was an extension of the study by Brezinsky [29]. This model gave very unsatisfactory results in CV calculations in comparison with Burcat's data. In addition to poor agreement with the measured ignition delay times, there were problems with convergence and this model was dropped from consideration.

The other benzene oxidation model that has recently been published is the study of Lindstedt and Skevis [30] which is based on the work of Bittker. Since the mechanisms were so similar, we did not do any comparison studies.

ZND Modeling

The ZND model and our previously developed implementation [20] using CHEMKIN [24, 31, 32] were used to compute reaction zone lengths for the benzene-air mixtures tested at McGill. STANJAN [16] was used to calculate the CJ velocity, temperature, and pressure. Only the CJ velocity is required as input for the ZND computation, the results of the ZND computation were checked by comparing the values of T and P at the end of the reaction zone with the CJ values.

Detonation parameters and reaction zone lengths are given in Table 1. Due to the limitations of the model, we were only able to compute reaction zone structures for equivalence ratios up to 1.9. For richer mixtures, the production of soot is quite evident in the experiments and outside the scope of our model for the chemical reactions.

Comparison (Fig. 11) between the measured cell widths and the calculated reaction zone length gave a proportionality factor A of 20. That is, the cell widths can be estimated as $\lambda = A\Delta_\sigma$. These results predict a cell width of about 50 mm for a stoichiometric composition, comparable to other hydrocarbon fuels such as propane. The computations only extend to an equivalence ratio of $\Phi = 1.9$, and are probably not reliable for values of Φ greater than 1.5. Under these fuel rich conditions, the experiments indicate the creation of a substantial amount of soot and the reaction model does not account for that.

Previous work on hydrocarbon-air mixtures has resulted in values of A ranging between 20 and 30 [19, 3] and extensive comparisons of λ and Δ_σ for the hydrogen-air-diluent system [20] have demonstrated that values between 10 and 60 can be obtained, depending on the diluent type and equivalence ratio. Our approach is strictly empirical since at the present time, there is no theoretical basis for predicting cell width for highly unstable fuel-air mixtures.

Parametric Study

A set of parametric computations have been carried out to determine the effect of composition, initial temperature and diluents on the reaction zone length. The results are shown in Figs. 12 to 16. The cases examined are:

1. Added hydrogen, hydrogen amount given as a fraction a of the total fuel, $a = 0$, .2, .4, .6, .8 and 1. Equivalence ratios Φ of 0.5, 1.0 and 1.5. Initial conditions: 20°C and 1 atm. The composition of the reactants was specified as

$$\Phi[a\mathrm{H_2} + (1\text{-}a)\mathrm{C_6H_6}] + X[\mathrm{O_2} + 3.76\mathrm{N_2}] \ .$$

   The value of X for stoichiometric compositions was computed for each value of a on the basis of complete combustion to CO_2 and H_2O.

   Up to a hydrogen fraction of 50%, the reaction zone length was essentially unchanged by the addition of hydrogen (Fig. 12). As the H_2 fraction was increased above 50%, the reaction zone length decreased sharply and is about 20 times smaller for pure H_2 compared to pure C_6H_6.

2. Initial temperature, 20 to 100°C. Benzene-air and C_6H_6-H_2-air mixtures, equivalence ratios of 0.5, 1.0 and 1.5. Initial pressure 1 atm. Reaction zone lengths decrease slightly with increasing initial temperature (Fig. 13). At 100°C, the reaction zone lengths are about 10% less than at 20°C for stoichiometric and rich mixtures, and about 40% less for the lean mixture.

3. Nitrogen dilution, 0 to 50%. Benzene-air and C_6H_6-H_2-air mixtures, equivalence ratios of 0.5, 1.0 and 1.5. Initial conditions: 20°C, 1 atm. Reaction zone lengths increase with increasing N_2 concentration (Fig. 14). The increase is more pronounced for the lean mixtures than for stoichiometric and rich mixtures.

4. Water vapor dilution at a fixed initial temperature of 90°C, 1 atm. Benzene-air and C_6H_6-H_2-air mixtures, equivalence ratios of 0.5, 1.0, and 1.5.

5. Water vapor dilution (90% of saturation concentration) with variable initial temperature 20 to 80°C, 1 atm. Benzene-air and C_6H_6-H_2-air mixtures, equivalence ratios of 0.5, 1.0 and 1.5. The reaction zone length increases with increasing water vapor concentration at both a fixed initial temperature (Fig. 15) or with a variable initial temperature (Fig. 16). Water vapor is slightly more effective as an inhibitor than nitrogen, but the effect is very similar. This indicates that the role of water is primarily as a thermal energy sink.

Conclusions

The present study indicates that as far as flame acceleration and transition to detonation are concerned, benzene behaves very similar to propane. The transition from slow turbulent flame to fast deflagration in the "choking" regime occurs at an equivalence ratio of about $\Phi \approx 0.65$ on the lean side and $\Phi \approx 1.8$ on the rich side. The fast deflagration in the choking regime travels at 700 to 900 m/s, close to the value of the sound speed of the burnt gases. For the present case of a blockage ratio of 0.43, DDT occurs at $\Phi \approx 0.88$ (lean) and $\Phi \approx 1.6$ (rich). Subsequent to DDT, the quasi-detonation velocity is of the order of 1450 m/s in the rough tube whereas the normal Chapman-Jouquet detonation speed is of the order of 1800 m/s in a smooth tube.

For the detonation sensitivity tests, cell sizes were measured over a range of compositions between 1.3% ($\Phi = 0.47$) to 6.75% ($\Phi = 2.58$) C_6H_6. At an equivalence ratio of $\Phi = 1$ (stoichiometric composition), the cell width for benzene-air mixture is about 66 mm compared to 50 mm for propane. Within the experimental error in the measurement of the cell size, we may conclude that benzene and propane are very similar as far as detonation sensitivity is concerned. The U-shaped curve of the cell size versus the equivalence ratio for benzene is wider than that of propane. The range of compositions for which DDT will occur is also wider in benzene than in propane.

A detailed chemical reaction scheme was used together with a numerical solution of the ZND model to estimate the reaction zone length. It was found that in the range of $0.5 \leq \Phi \leq 1.2$ the cell width was about 20 times the computed ZND reaction zone length. The kinetic model breaks down for rich mixtures, $\Phi \geq 1.5$.

References

1. Moen, I. O., *J. Hazardous Matl.* 33:159 (1993).

2. Beeson, H. D., McClenagan, R. D., Bishop, C. V., Benz, F. J., Pitz, W. J., Westbrook C. K. and Lee J. H. S. in *Prog. Astronaut. Aeronaut.* 133:19 (1991).

3. Tieszen, S. R., Stamps, D. W., Westbrook, C. K. and Pitz, W. J., *Combust. and Flame* 84:376 (1991).

4. Peraldi, O., Knystautas, R. and Lee, J. H. S., *Twenty-first Symposium (International) on Combustion,* The Combustion Institute, Pittsburgh, PA, 1986, p. 1629.

5. Lee, J. H., Knystautas, R. and Chan, C. K., *Twentieth Symposium (International) on Combustion,* The Combustion Institute, Pittsburgh, PA, 1984, p. 1663.

6. Chue, R. S., Clarke, J. F. and Lee, J. H., *Proc. Roy. Soc. Lond.* A 441:607 (1993).

7. Zeldovich, Ya. B. and Kompaneets, A. S., *Theory of Detonation*, Academic Press, New York, 1960, p. 109.

8. Taylor, G. I. and Tankin, R. S. in *Fundamentals of Gasdynamics* (H. W. Emmons, Ed.), Princeton University Press, 1958, p. 622.

9. Lee, J. H. S. and Moen. I. O. *Prog. Energy Combust. Sci.* 6:359 (1980).

10. Teodorczyk, A., Lee, J. H. S. and Knystautas, R., *Twenty-second Symposium (International) on Combustion,* The Combustion Institute, Pittsburgh, PA, 1988, p. 1723.

11. Chan, C. K. and Greig, D. R. *Twenty-second Symposium (International) on Combustion,* The Combustion Institute, Pittsburgh, PA, 1988, p. 1733.

12. Moen, I. O., Sulmistras, A., Thomas, G. O., Bjerketvedt, D. and Thibault, P. A. in *Prog. Astronaut. Aeronaut.* 106:220 (1986).

13. Lee, J. H. S., *Annu. Rev. Fluid Mech.* 16:311 (1984).

14. Guirao, C. M., Knystautas, R., Lee, J. H. S., Benedick, W. B. and Berman, M., *Nineteenth Symp. (International) Combust.*, The Combustion Institute, Pittsburgh, PA, 1982, p. 635.

15. Guirao, C. M., Knystautas, R. and Lee, J. H. S., *A Summary of Hydrogen-Air Detonation Experiments,* Sandia National Laboratories Report SAND87-7128 (NUREG/CR-4961), 1989.

16. Reynolds, W. C., *The Element Potential Method for Chemical Equilibrium Analysis: Implementation in the Interactive Program STANJAN,* Version 3., Dept. of Mechanical Engineering, Stanford, CA, January 1986.

17. Knystautas, R., Guirao, C., Lee, J. H. and Sulmistras, A., in *Prog. Astronaut. Aeronaut.* 94:23 (1984).

18. Bull, D. C., Ellsworth, J. E. and Schuff, P. J., *Combust. and Flame* 45:7 (1982).

19. Westbrook, C. K. and Urtiew, P. A., *Nineteenth Symposium (International) on Combustion,* The Combustion Institute, Pittsburgh, PA, 1982, p. 615.

20. Shepherd, J. E. in *Prog. Astronaut. Aeronaut.* 106:263 (1986).

21. Bittker, D. A., *Detailed Mechanism of Benzene Oxidation,* NASA Technical Memorandum 100202, 1987.

22. Bittker, D. A., *Detailed Mechanism for Oxidation of Benzene,* NASA Technical Memorandum 102443, 1990.

23. Bittker, D. A., *Combust. Sci. and Technol.* 79:49 (1991).

24. Kee, R. J., Rupley, F. M., Miller, J. A., *The Chemkin Thermodynamic Data Base,* Sandia National Laboratories Report SAND87–8215, 1987.

25. Burcat A., Zeleznik, F. J., and McBride, B. J., *Ideal Gas Thermodynamic Properties for the Phenyl, Phenoxy, and o-BiPhenyl Radicals,* NASA Technical Memorandum 83800, 1985.

26. Burcat, A., McBride, B. J., *1995 Ideal Gas Thermodynamic Data for Combustion and Air-Pollution Use,* Technion - Israel Institute of Technology, Report No. TAE 697, 1995.

27. Burcat, A., Snyder, C., and Brabbs, T., *Ignition Delay Times of Benzene and Toluene with Oxygen in Argon Mixtures,* NASA Technical Memorandum 87312, 1986.

28. Emdee, J. L., Brezinsky, K. and Glasman, I., *J. Phys. Chem.* 96:2151 (1992).

29. Brezinsky, K., *Prog. Energy Combust. Sci.* 12:1 (1986).

30. Lindstedt, R. P. and Skevis, G., *Combust. Flame* 99:551 (1994).

31. Kee, R. J., Miller, J. A., Jefferson, T. H., *CHEMKIN: A General–Purpose, Problem–Independent, Transportable, Fortran Chemical Kinetics Code Package,* Sandia National Laboratories Report SAND80–8003, 1980.

32. Kee, R. J., Rupley, F. M., and Miller, J. A., *Chemkin-II: A Fortran Chemical Kinetics Package for the Analysis of Gas-Phase Chemical Kinetics,* Sandia National Laboratories Report SAND89–8009, 1989.

Table 1: Detonation parameters for C_6H_6-air mixtures.

Φ	C_6H_6 (%)	U_{CJ} (m/s)	T_{CJ} (K)	P_{CJ} (bar)	Δ_σ (mm)	c_f (m/s)
.4	1.11	1397.	1843.	10.7	469.	704.
.5	1.38	1504.	2121.	12.5	89.	752.
.6	1.65	1593.	2366.	14.2	28.1	795.
.7	1.92	1662.	2567.	15.6	12.8	830.
.8	2.19	1715.	2719.	16.9	7.3	855.
.9	2.46	1754.	2825.	17.8	5.0	870.
1.	2.72	1783.	2895.	18.5	3.8	880.
1.1	2.99	1805.	2935.	19.	3.2	892.
1.2	3.25	1819.	2949.	19.3	2.8	903.
1.3	3.51	1827.	2937.	19.5	2.7	907.
1.4	3.77	1828.	2901.	19.4	2.7	904.
1.5	4.03	1824.	2846.	19.2	2.8	898.
1.6	4.29	1815.	2778.	19.	3.0	891.
1.7	4.55	1802.	2704.	18.7	3.3	884.
1.8	4.8	1788.	2626.	18.4	3.7	876.
1.9	5.05	1773.	2548.	18.1	4.2	868.
2.0	5.31	1757.	2470.	17.8	-	859.
2.1	5.56	1740.	2392.	17.5	-	851.
2.2	5.80	1721.	2314.	17.2	-	842.
2.3	6.05	1702.	2237.	16.8	-	832.

Table 2: Detonation cell width for stoichiometric hydrocarbon-air mixtures. Data from Tieszen *et al.* [3] except benzene. Initial conditions were 25°C and 1 atm, except for hexane, octane, JP4, and decane data which were obtained at 100°C.

Fuel		λ (mm)
Methane	CH_4	340
Hydrogen	H_2	10
Acetylene	C_2H_2	5.3
Ethylene	C_2H_4	19.5
Ethane	C_2H_6	50
Propane	C_3H_8	50
Benzene	C_6H_6	66
Hexane	C_6H_{14}	55
Octane	C_8H_{18}	42
JP4	-	45
Decane	$C_{10}H_{22}$	42

Figures

1. Flame velocity vs distance along the 15-cm-diameter tube (orifice plates, BR = 0.43, spacing 15 cm) for several benzene-air and propane-air mixtures.

2. Terminal Flame velocity vs composition in the 15-cm-diameter tube (orifice plates every 15 cm) for propane-air mixtures. BR = 0.43 data are from the present study, BR =0.39 data are from Peraldi *et al.* [4].

3. Terminal Flame velocity or detonation velocity vs composition in the 15-cm-diameter tube (BR = 0.43 orifice plates every 15 cm) for benzene-air mixtures. Lean mixtures with 1 and 5% H_2 are also shown.

4. Detonation cell width λ vs composition (volume % of fuel in the fuel-air mixture) for benzene-air and propane-air mixtures.

5. Detonation cell width λ vs composition (equivalence ratio) for benzene-air and propane-air mixtures.

6. Comparison between the shock-tube data of Burcat and the computed constant volume explosion time using the modified Bittker model. Composition: $1.69C_6H_6$ + $12.675O_2$ + 85.63Ar; initial conditions: 293.15 K, 2.04 – 3.01 bar.

7. Comparison between the shock-tube data of Burcat and the computed constant volume explosion time using the modified Bittker model. Composition: $1.35C_6H_6$ + $5.09O_2$ + 93.55Ar; initial conditions: 293.15 K, 2.04 – 3.01 bar.

8. Comparison between the shock-tube data of Burcat and the computed constant volume explosion time using the modified Bittker model. Composition: $1.35C_6H_6$ + $20.31O_2$ + 78.33Ar; initial conditions: 293.15 K, 1.90 – 2.73 bar.

9. Comparison between the shock-tube data of Burcat and the computed constant volume explosion time using the modified Bittker model. Composition: $0.419C_6H_6$ + $12.57O_2$ + 87.01Ar; initial conditions: 293.15 K, 1.69 – 2.40 bar.

10. Comparison between the shock tube data of Burcat and the computed constant volume explosion time using the modified Bittker model. Composition: $0.516C_6H_6$ + $3.87O_2$ + 95.62Ar; initial conditions: 293.15 K, 5.69 – 7.89 bar.

11. Comparison between 150-mm-diameter tube data for detonation cell width and the scaled ($A = 20$) ZND model results for benzene-air mixtures. Initial conditions: 293.15 K, 1 atm.

12. Effect of hydrogen fraction a (in total fuel) on estimated cell widths ($A = 20$) for benzene-hydrogen air mixtures at three equivalence ratios, F = 0.5, 1.0, 1.5. Initial conditions: 293.15 K, 1 atm.

13. Effect of initial temperature on estimated cell widths ($A = 20$) for benzene-air mixtures (solid symbols) and equimolar benzene-hydrogen (open symbols) with air. Initial conditions: 293.15 K, 1 atm.

14. Effect of nitrogen dilution on estimated cell widths ($A = 20$) for benzene-air mixtures (solid symbols) and equimolar benzene-hydrogen (open symbols) with air. Initial conditions: 293.15 K, 1 atm.

15. Effect of water (steam) on estimated cell widths ($A = 20$) for benzene-air mixtures (solid symbols) and equimolar benzene-hydrogen (open symbols) with air. Initial conditions: 363.15 K, 1 atm.

16. Effect of water (steam) on estimated cell widths ($A = 20$) for benzene-air mixtures (solid symbols) and equimolar benzene-hydrogen (open symbols) with air. Initial conditions: variable initial temperature 20 to 80 C, 1 atm, steam concentration 90% of saturation.

Figure 1: Knystautas, Lee, Teodoczyk, Shepherd

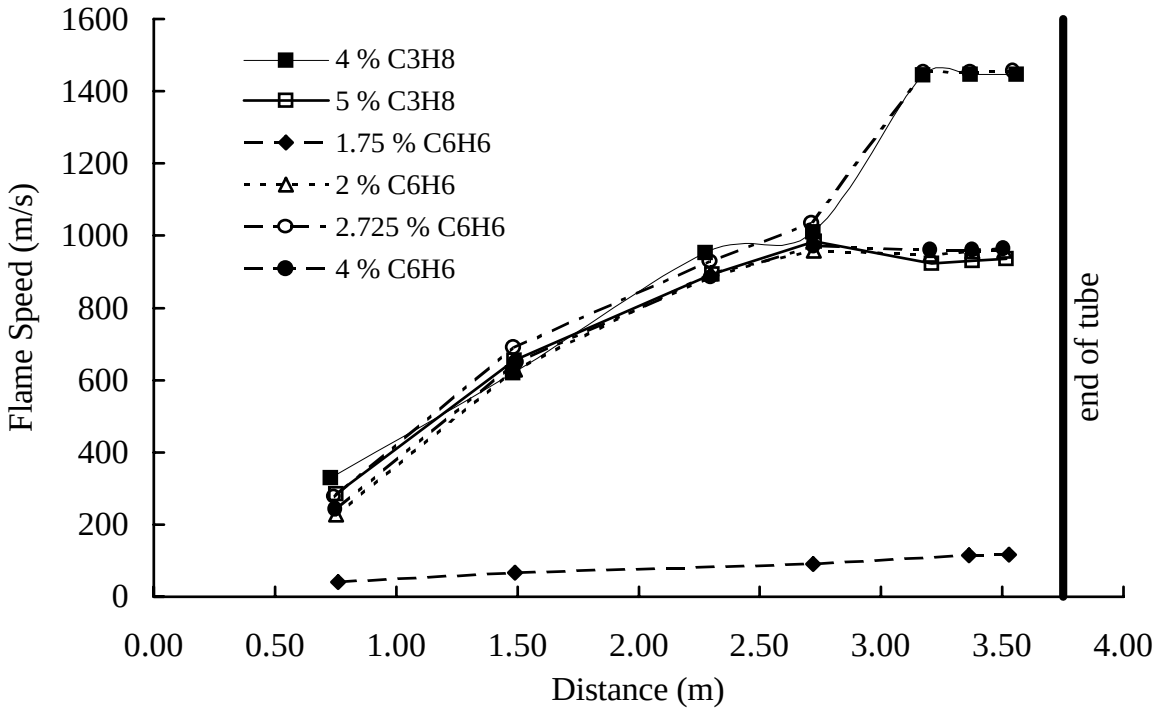

Figure 2: Knystautas, Lee, Teodoczyk, Shepherd

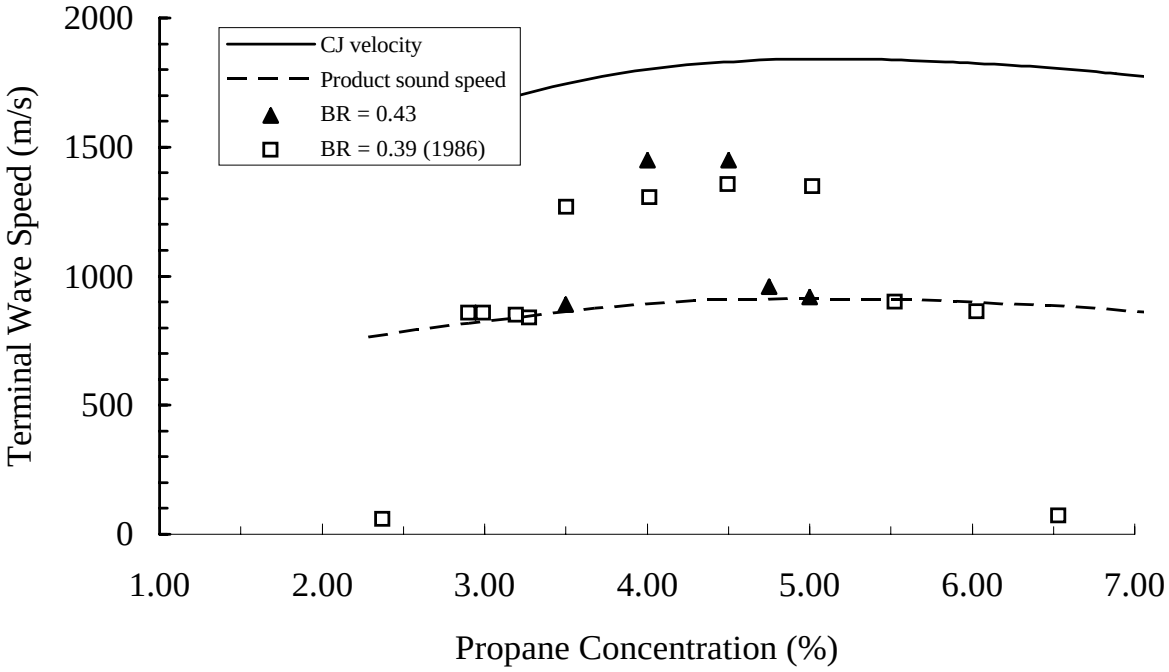

Figure 3: Knystautas, Lee, Teodoczyk, Shepherd

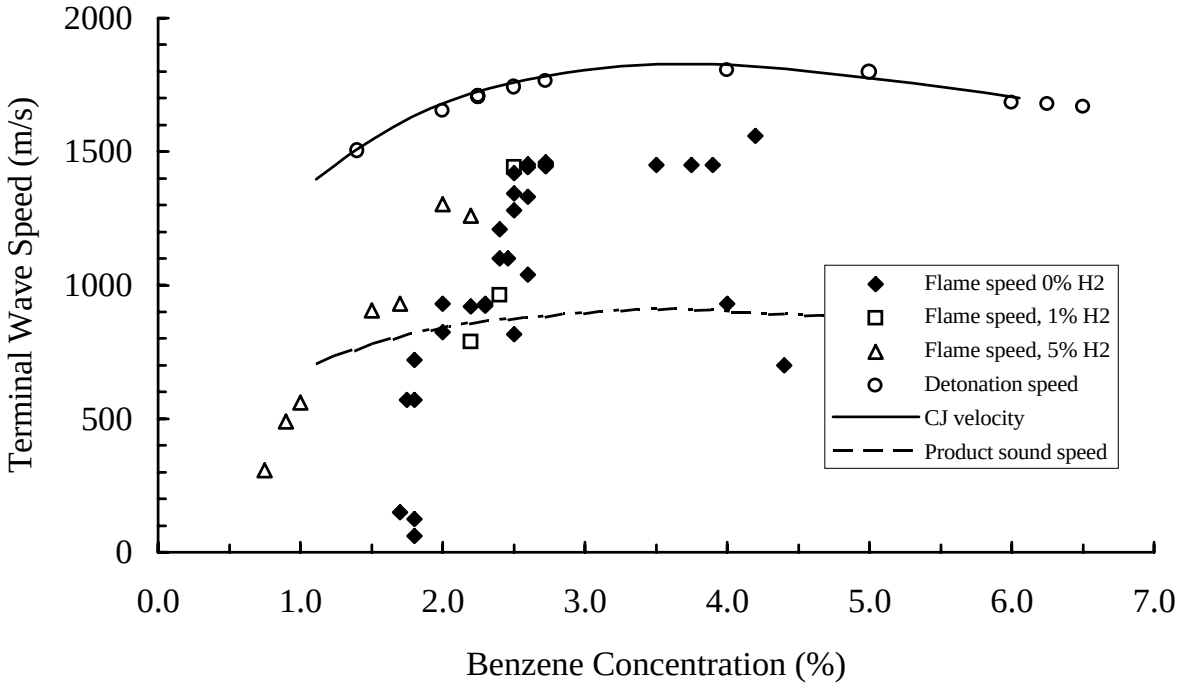

Figure 4: Knystautas, Lee, Teodoczyk, Shepherd

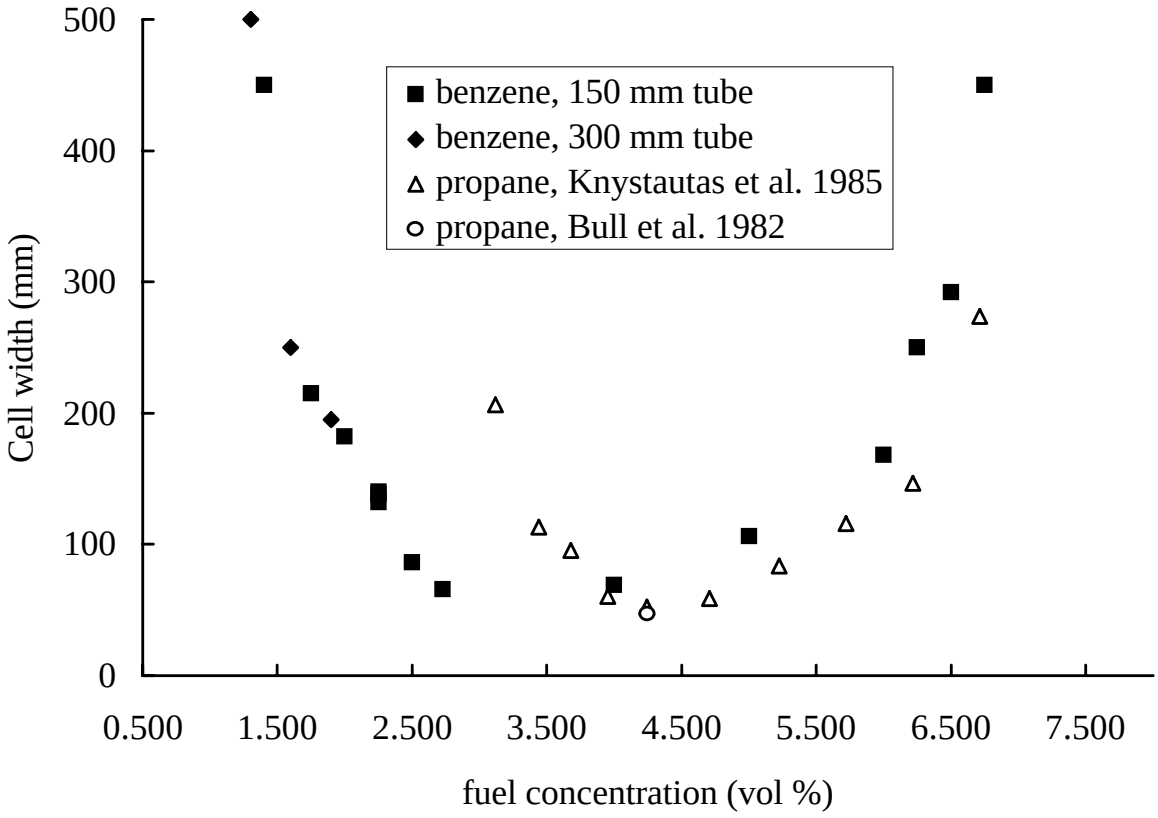

Figure 5: Knystautas, Lee, Teodoczyk, Shepherd

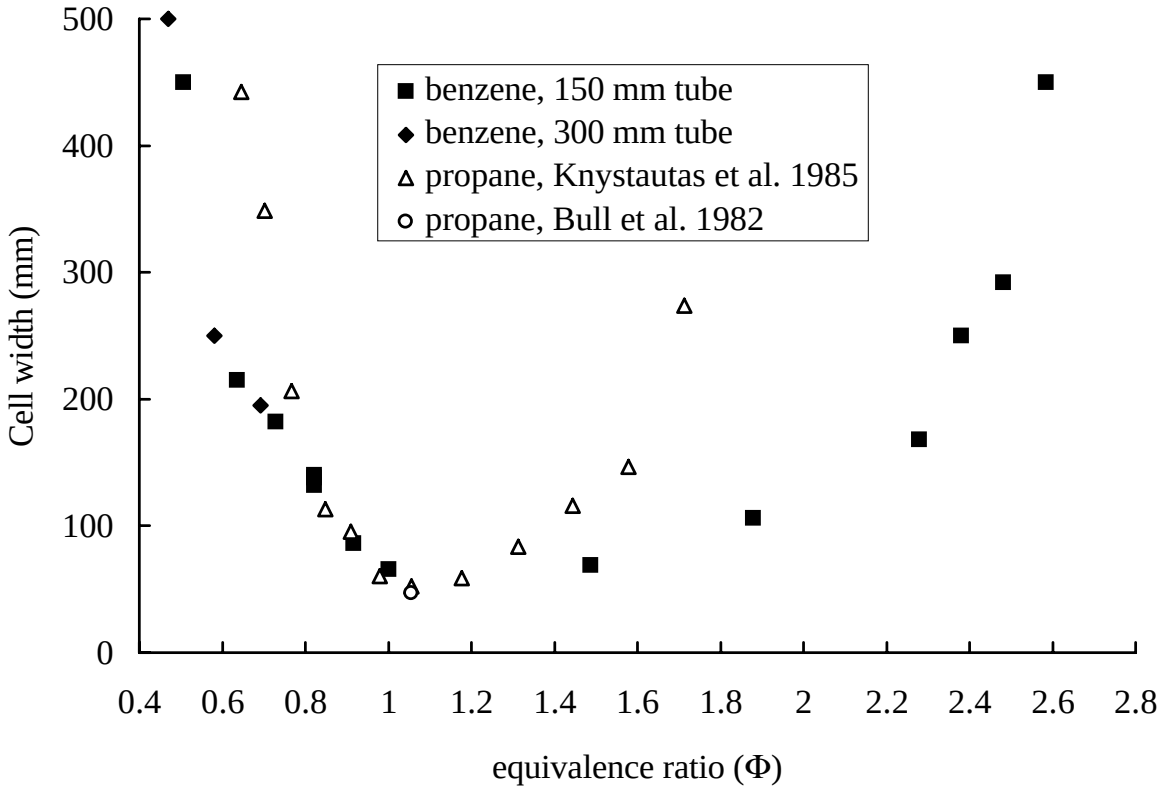

Figure 6: Knystautas, Lee, Teodoczyk, Shepherd

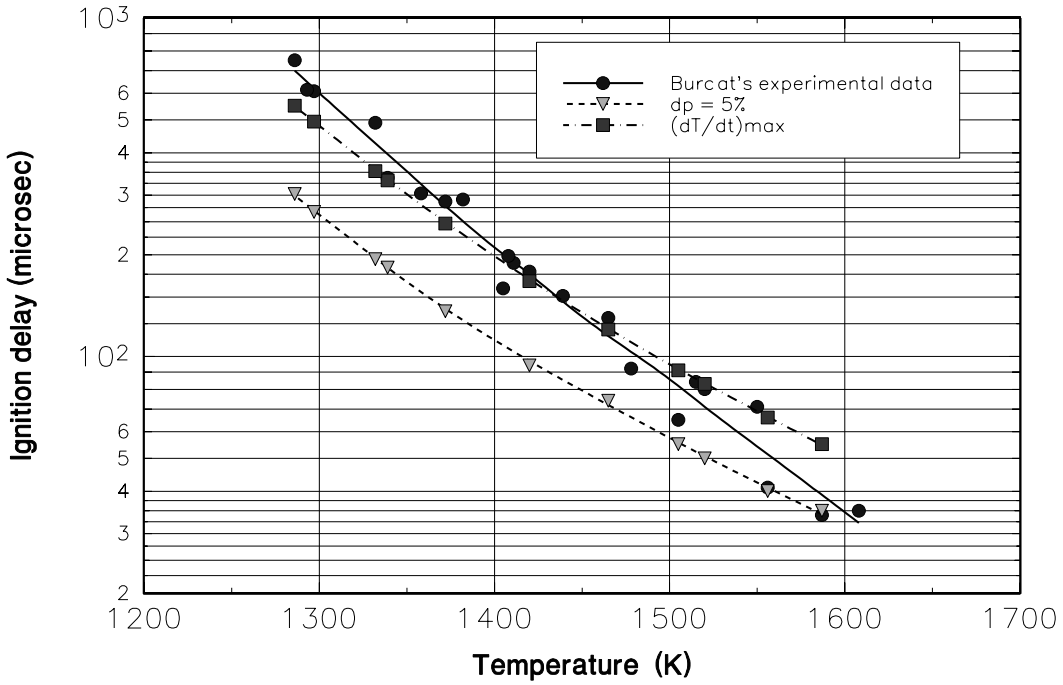

Figure 7: Knystautas, Lee, Teodoczyk, Shepherd

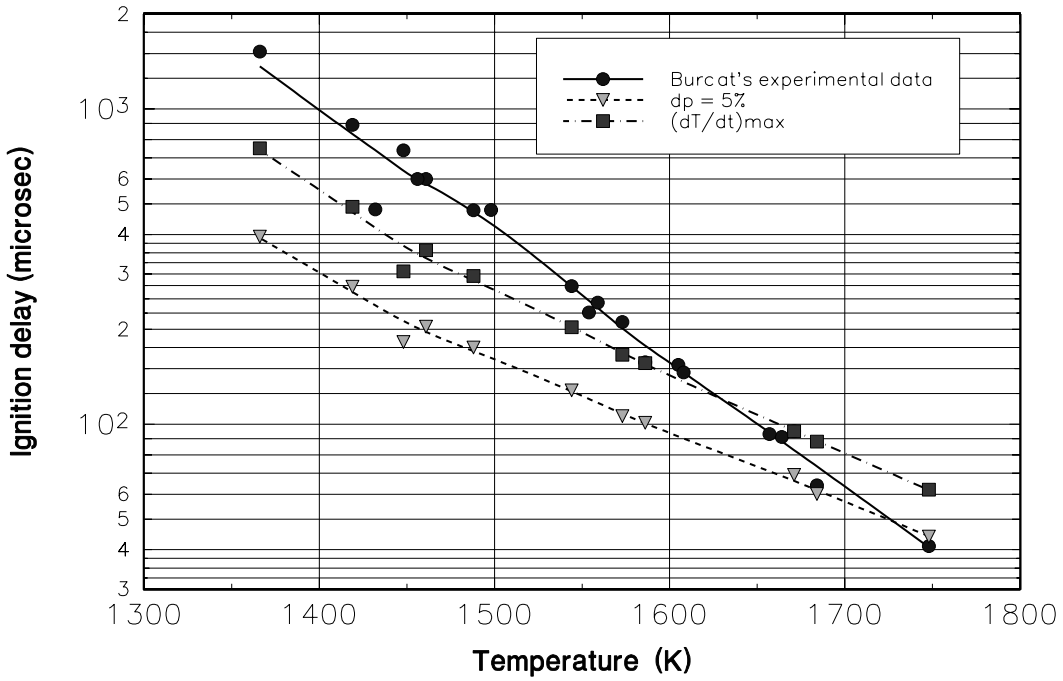

Figure 8: Knystautas, Lee, Teodoczyk, Shepherd

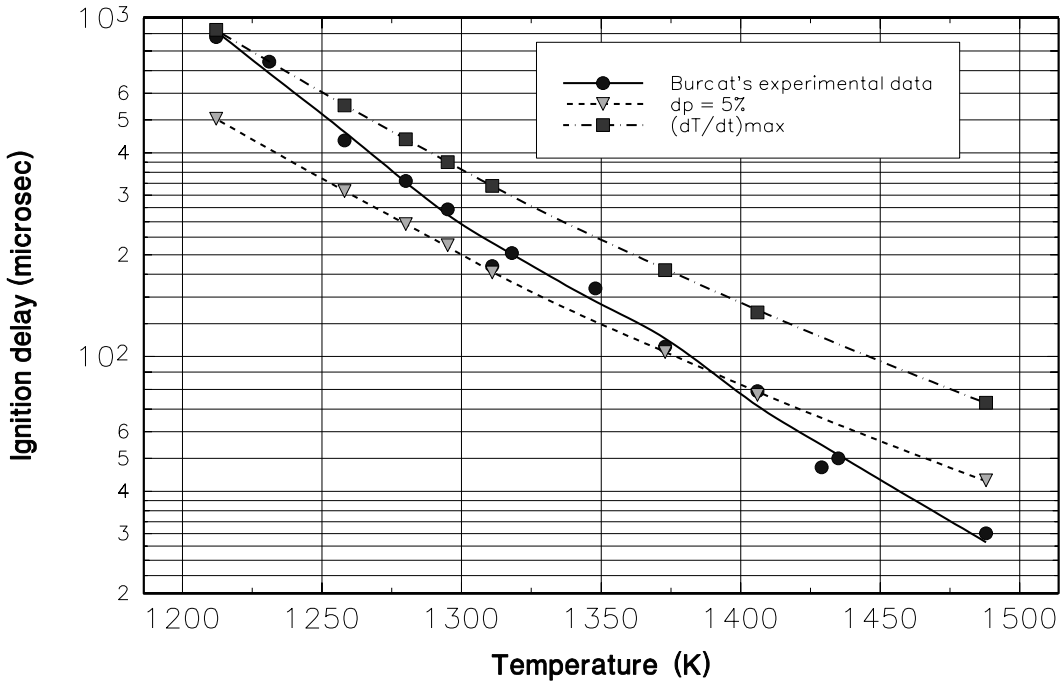

Figure 9: Knystautas, Lee, Teodoczyk, Shepherd

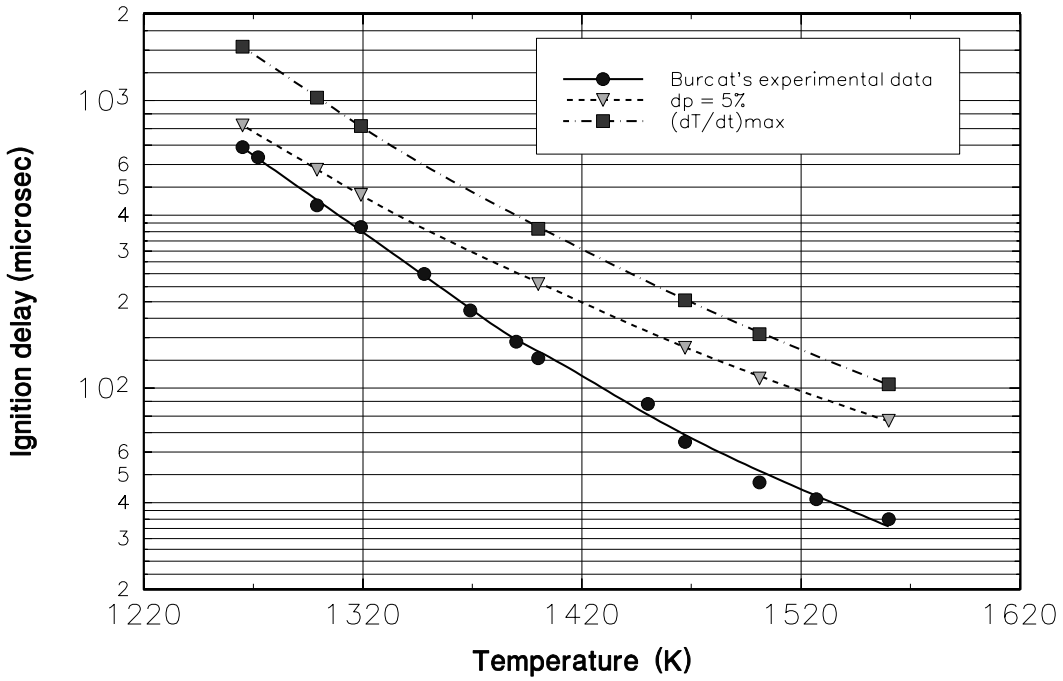

Figure 10: Knystautas, Lee, Teodoczyk, Shepherd

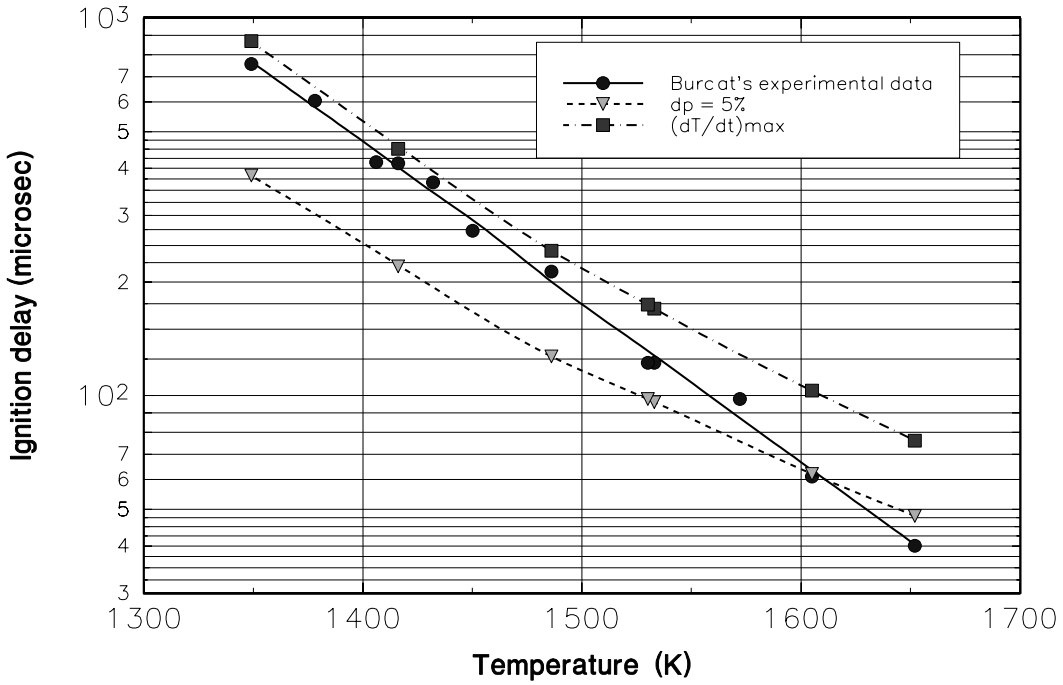

Figure 11: Knystautas, Lee, Teodoczyk, Shepherd

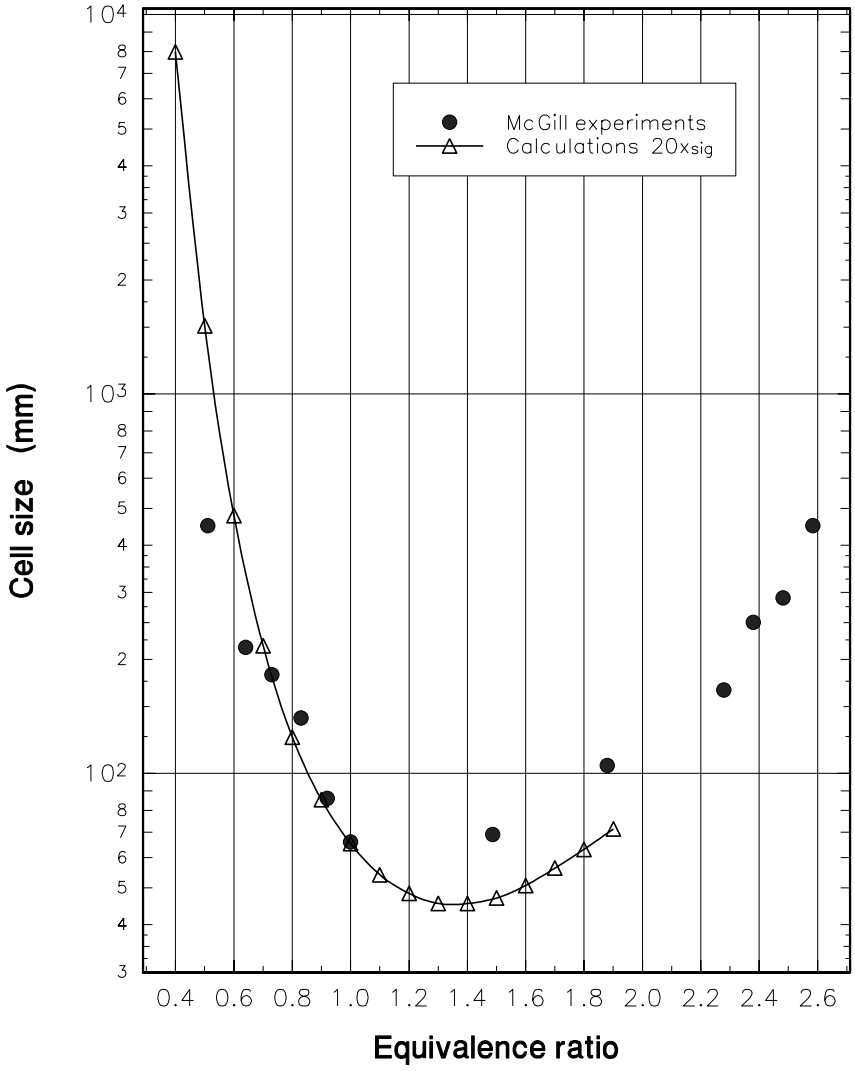

Figure 12: Knystautas, Lee, Teodoczyk, Shepherd

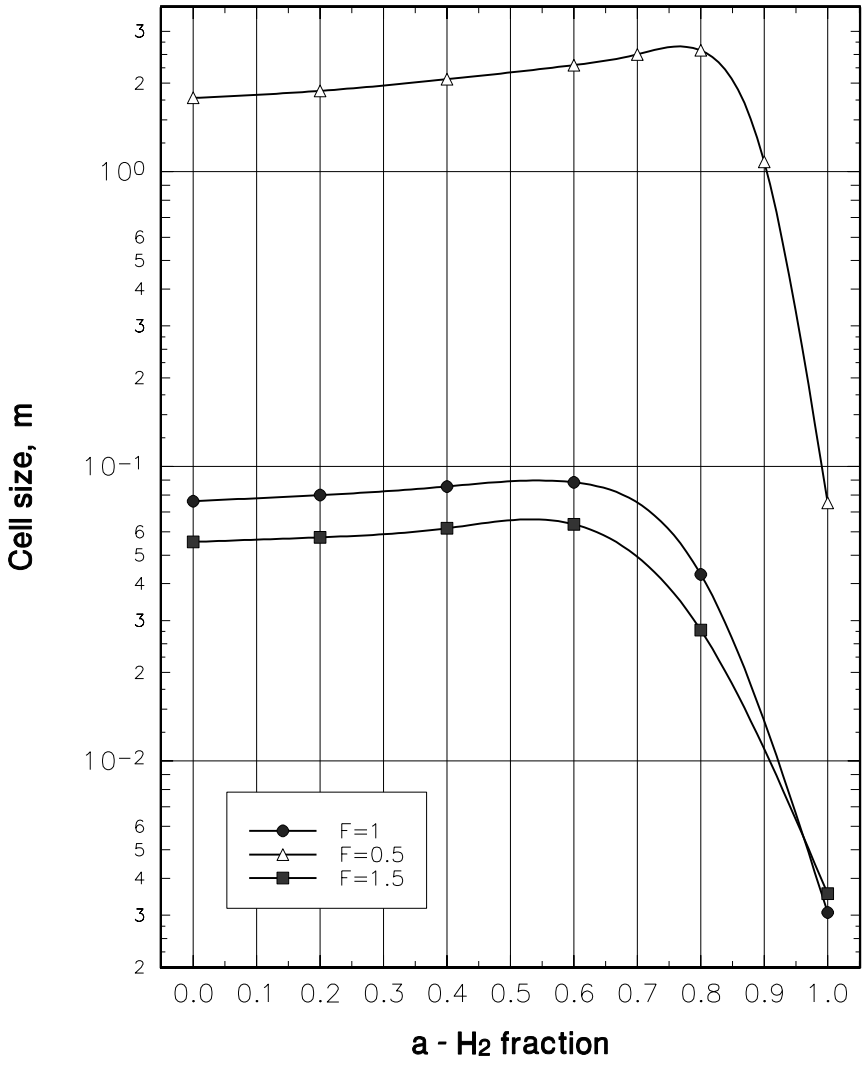

Figure 13: Knystautas, Lee, Teodoczyk, Shepherd

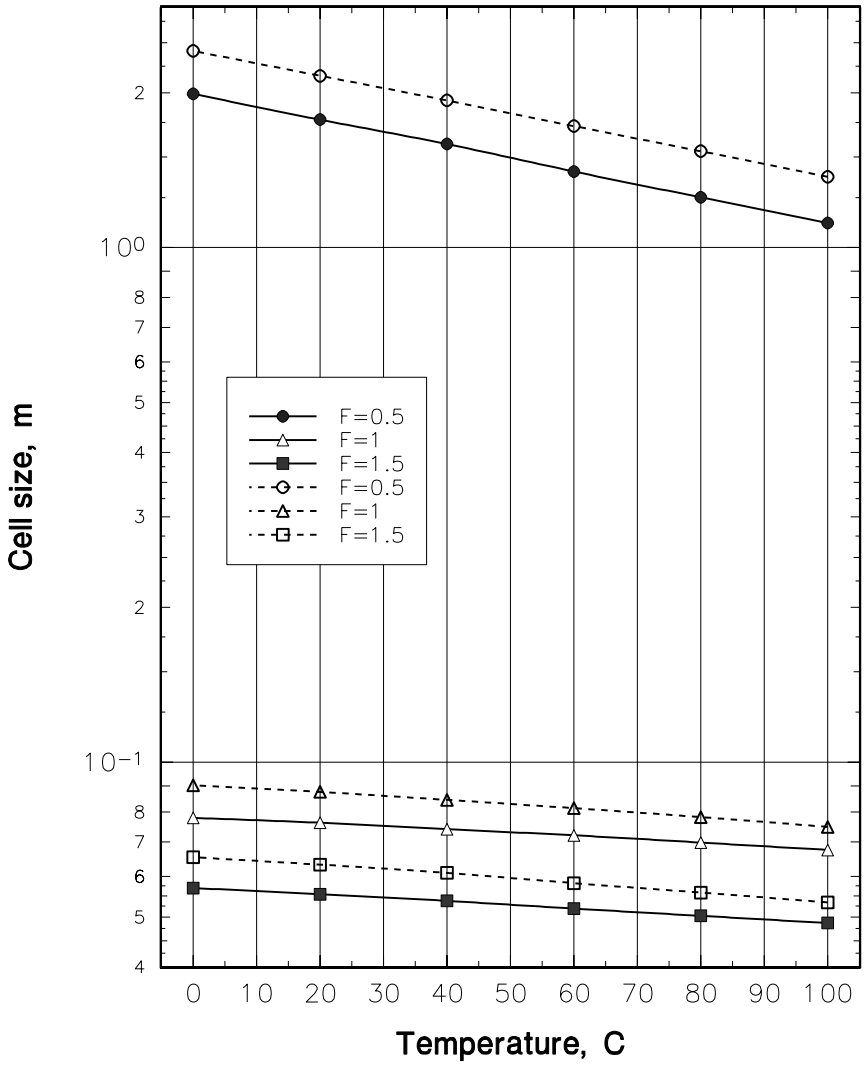

Figure 14: Knystautas, Lee, Teodoczyk, Shepherd

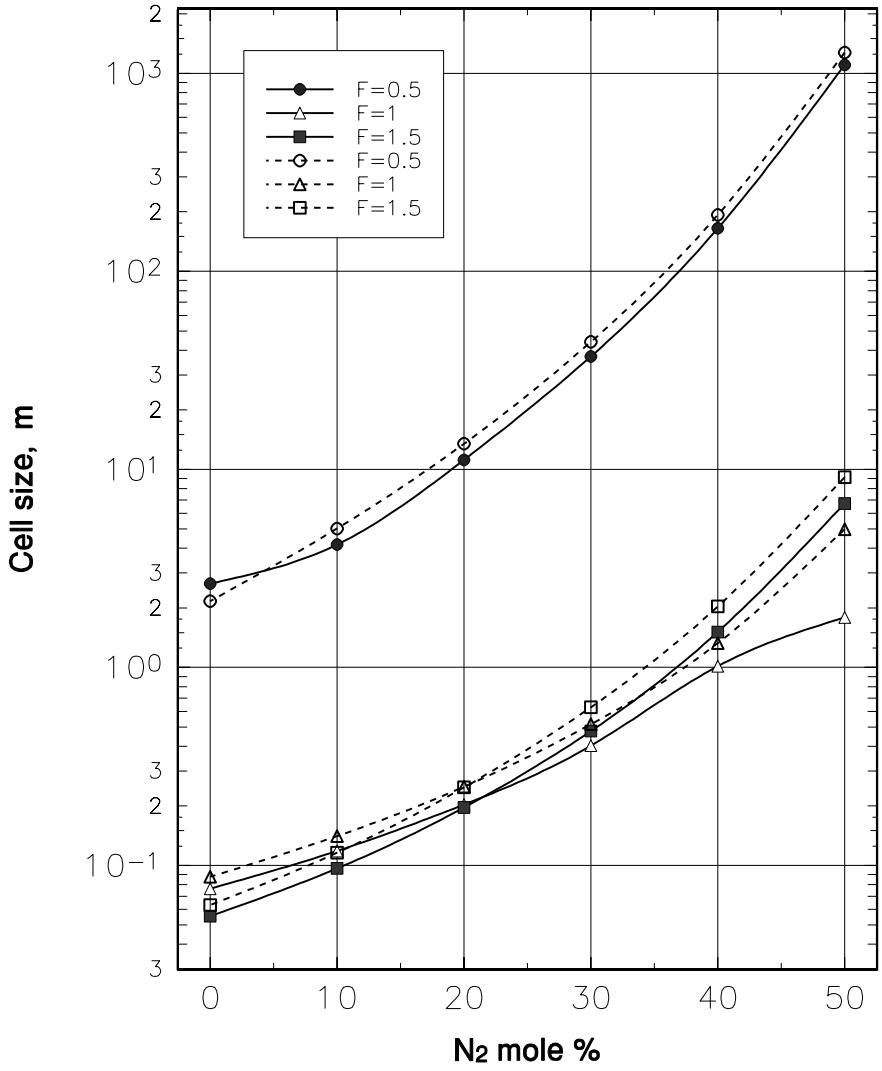

Figure 15: Knystautas, Lee, Teodoczyk, Shepherd

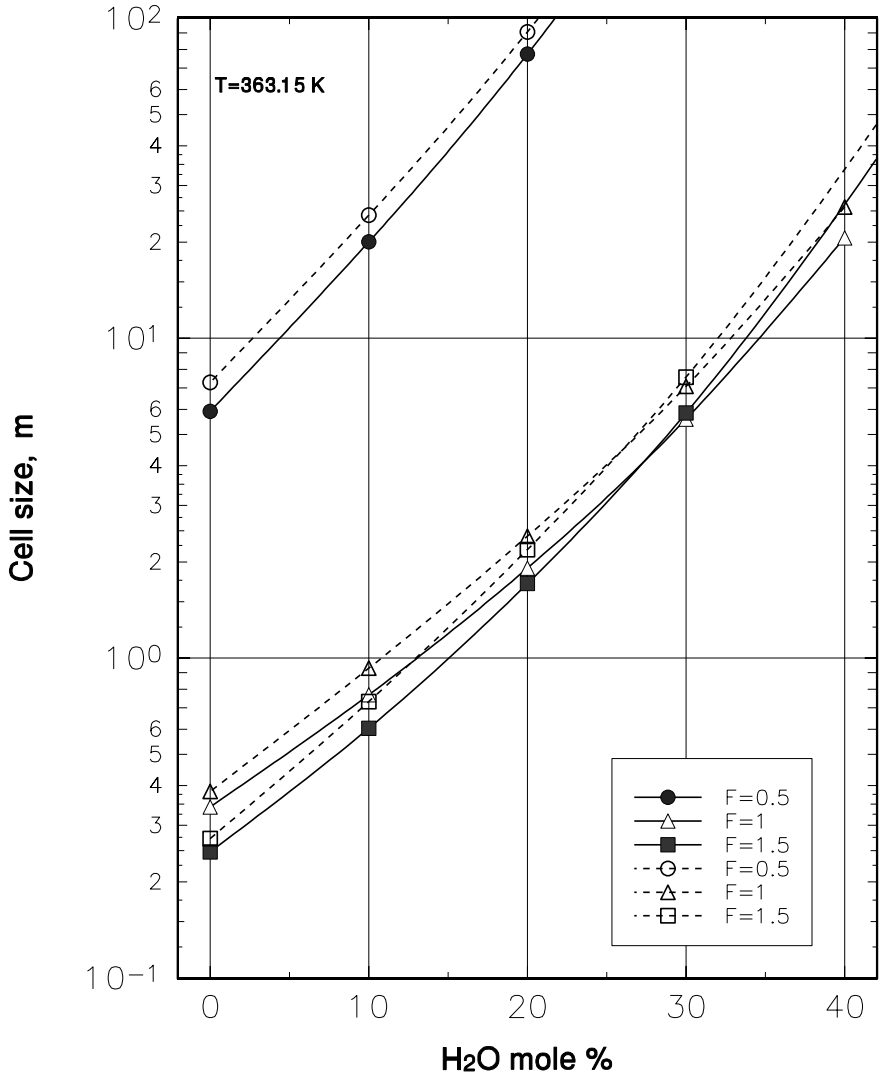

Figure 16: Knystautas, Lee, Teodoczyk, Shepherd